

The Hall Effect and ionized impurity scattering in $\text{Si}_{(1-x)}\text{Ge}_x$

P. Kinsler[*]

Department of Physics, Imperial College, Prince Consort Road, London SW7 2BW, United Kingdom.

W.Th. Wenckebach

*Department of Applied Physics, Technical University Delft,
Lorentzweg 1, 2628 CJ DELFT, The Netherlands.*

(Dated: May 22, 2019)

Using Monte Carlo simulations, we demonstrate that including ionized impurity scattering in models of $\text{Si}_{(1-x)}\text{Ge}_x$ is vital in order to predict the correct Hall parameters. Our results show good agreement with the experimental data of Joelsson et.al. [1].

This is a draft of a paper submitted to the Journal of Applied Physics.

ulations for linearly interpolated band parameters with experiments. Finally in section IV we present our conclusions.

I. INTRODUCTION

There is much current interest in using Si/Ge strained layer superlattices and multiple quantum wells to fabricate optoelectronic and electronic devices – one example being better high frequency performance for heterojunction bipolar transistors. In order to design effective devices we need to know the carrier concentration N_H and the conduction mobility μ_c , which are usually obtained using Hall measurements. However, to extract N_H and μ_c from the experimental results, we need to know the Hall coefficient r_H – but experiments in $\text{Si}_{(1-x)}\text{Ge}_x$ [1, 2] have shown r_H has values that cannot be accounted for by existing attempts at modelling (see e.g. [3, 4]). Also, the Hall factor r_H allows an interesting test of the accuracy of the band parameters because it is quite sensitive to both the non-parabolicity and anisotropy of the bands.

The reason that Hall data from existing experiments [1, 2] is not well explained by existing models is most probably either because (a) these models used a linearly interpolated bandstructure, or (b) they omitted the important effects of ionised impurity scattering. Alternatives to a linearly interpolated bandstructure have been given by Rieger and Vogl [5], using an empirical pseudopotential approach, and Hayes suggests a similar method based on results of a parallelized Car-Parrinello scheme [6]. Some other papers discussing models and bandstructure parameters for SiGe alloys are [7, 8, 9].

Here we attack the second of these shortcomings, by calculating the Hall parameters using a comprehensive Monte Carlo simulation of hole motion in $\text{Si}_{(1-x)}\text{Ge}_x$ strained to a silicon substrate. These simulations are aided by the incorporation of a new optimised scheme for treating ionised impurity scattering[10]. Our results show that the inclusion of ionised impurity scattering successfully explains the experimental data, leaving the bandstructure interpolation as a secondary effect.

The paper is organised as follows: section II describes the Monte Carlo model used in the mobility and Hall calculations; section III compares the results of the sim-

II. THE MONTE CARLO MODEL

Our Monte Carlo simulations[11] of this system include a full $k.p$ band structure calculation [12] and all important scattering processes: optical and acoustical deformation potential, alloy, and (in particular) ionised impurity scattering[13, 14]. We treat the effect of the electric and magnetic fields classically, giving the holes continuous trajectories in k -space – comparison with experiment for p-Ge systems indicates that this approximate treatment is adequate for the field strengths we consider. We used a similar Monte Carlo model recently for studies of hot hole lasers[15, 16]. All simulations are done at a lattice temperature of 300K. They follow the progress of a single hole through a large number of scatterings (typically $\sim 10^6 \times 100$), with the ergodic theorem being used to justify the use of the time-average as an ensemble average. Often a very large number of scatterings was needed in order to make sure the statistical errors in the Hall parameter were small enough. Our material parameters are listed in table I.

The Monte Carlo simulations used the standard overestimation technique where for each scattering process the post-scattering direction of the hole was chosen at random, and the differential scattering rate was overestimated by an isotropic rate just higher than its maximum value. Normally this would be very slow for the ionised impurity scattering, especially at low impurity concentrations. Consequently, we use an optimised scheme [10] that weights the choice of scattering angle by the angular dependence of the scattering rate, and thus avoid generating a large proportion of inefficient overestimations.

III. RESULTS

The Hall co-efficient r_H is very sensitive to both the shape and non-parabolicity of the bandstructure, as well as the anisotropy of the scattering processes. This means

that the role of ionised impurity scattering can be crucial – not only the presence or absence of impurities makes a difference; different impurity concentrations can produce Hall factors that vary with alloy concentration in both quantitatively and qualitatively different ways. As a result we need to compare our simulation results with experiment to ascertain whether our model is sufficiently accurate and include all the necessary important features.

Experimental results for the Hall factor in relaxed SiGe have been reported by Chen et.al. [2] for impurity concentrations of about $n \sim 10^{17}\text{cm}^{-3}$; and in SiGe strained to a Si substrate by Joelsson et.al. [1] for $n \sim 10^{18}\text{cm}^{-3}$. A comparison of these experimental results with Monte Carlo simulations has been done by Dijkstra [3, 4], whose simulations used linearly interpolated band parameters and neglected ionised impurity scattering. We have done equivalent simulations to those of Dijkstra, and include the results here.

To calculate the Hall factor, we use the efficient estimator of the Hall mobility μ_H presented by [3, 17],

$$\mu_H = \frac{\langle \vec{v} \cdot (\vec{r} \times \vec{B}) \rangle}{\langle (\vec{v} \times \vec{B}) \cdot (\vec{r} \times \vec{B}) \rangle}, \quad (3.1)$$

and then since $r_H = \mu_H/\mu_c$, the drift mobility is

$$\mu_c = \frac{e}{k_B T} \frac{1}{2|\vec{B}|^2} \langle (\vec{v} \times \vec{B}) \cdot (\vec{r} \times \vec{B}) \rangle. \quad (3.2)$$

We did our simulations with no electric field, and a magnetic field in the [001] direction, in accordance with experiment; magnetic field strengths of $B = 0.30, 1.00$, or 2.00T were investigated. We used a strain equivalent to that as if the $\text{Si}_{1-x}\text{Ge}_x$ alloy had been grown as an epitaxial layer on a (001)Si substrate. This means the usual strain parameter $\epsilon_{zz} > 0$, since the lattice parameter of Si is smaller than that for Ge.

Our alloy scattering potential was $U_0 = 0.51\text{eV}$. Note that some authors [8, 9], on the basis of fits to mobilities and other transport parameters, prefer a stronger alloy scattering potential ($\sim 1\text{eV}$); other discussions of the effect of alloy potential (and high impurity concentrations) can be found in [18, 19]. We do not expect our results for r_H to be particularly sensitive to the strength of the alloy potential, as alloy scattering is isotropic. This assumption was confirmed by a set of simulations on undoped SiGe using the Monte Carlo program of Dijkstra[3]. However, we would expect the drift mobility to diminish for higher concentrations of germanium if a stronger alloy scattering potential were chosen.

Comparison with experimental results can be seen on fig. 1, where those for $\sim 2.5 \times 10^{18}\text{cm}^{-3}$ (\bullet) and $\sim 7 \times 10^{18}\text{cm}^{-3}$ (\star) show a Hall coefficient decreasing as the Ge content increases. These clearly do not agree with our undoped Monte Carlo simulations at 0.3T (\square), although Monte Carlo simulations at the higher field of 2T (\triangle) do also have dip at low-Ge fraction. This dip at

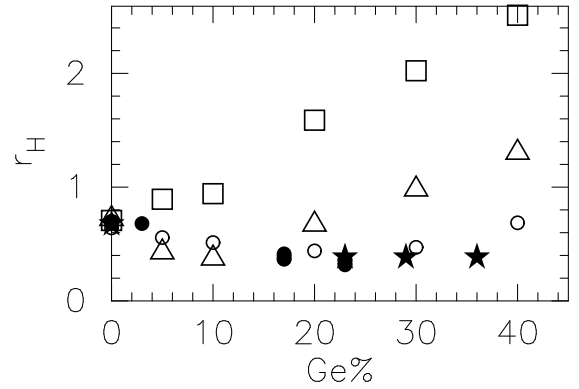


FIG. 1: Hall coefficient comparison with experiment[1] for strained $\text{Si}_{1-x}\text{Ge}_x$ alloy, at $B = 0.30\text{T}$, as a function of Ge fraction. **Monte Carlo:** \square = undoped; \circ = $3.16 \times 10^{18}\text{cm}^{-3}$; \triangle = undoped 2T ; **Experiment[1]:** \bullet = 2.08 – $2.98 \times 10^{18}\text{cm}^{-3}$; \star = 6.59 – $7.65 \times 10^{18}\text{cm}^{-3}$; Error bars are not included because the symbols become obscured, but all simulation errors are listed in table II.

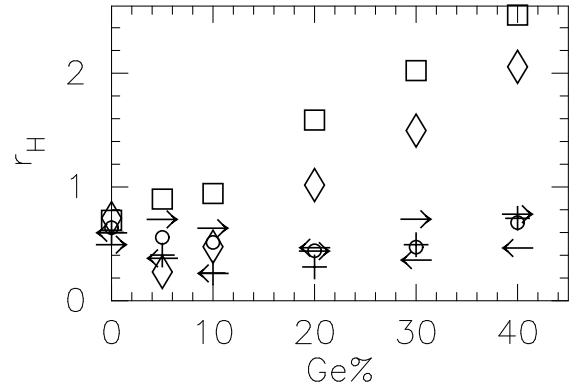


FIG. 2: Hall coefficients for strained $\text{Si}_{1-x}\text{Ge}_x$ alloy, at $B = 0.30\text{T}$, as a function of Ge fraction. **Monte Carlo:** \square = undoped; \diamond = 10^{15}cm^{-3} ; $+$ = 10^{17}cm^{-3} ; \leftarrow = 10^{18}cm^{-3} ; \circ = $3.16 \times 10^{18}\text{cm}^{-3}$; \rightarrow = 10^{19}cm^{-3} . Error bars are not included because the symbols become obscured, but are listed in table II.

2T has been previously reported for Monte Carlo simulations without ionised impurity scattering [3, 4]. However, the 2T simulations have a minimum r_H at 15% Ge, with a subsequent increase – at 40% Ge r_H is well above 1. This is contrary to experiments, where r_H continues to decrease up to 36% Ge.

However, it is clear that for undoped SiGe (fig. 1, \square), there is no dip like that seen in experiments on doped material – hence, results for undoped SiGe do *not* explain the experiment. Our simulations with $B = 0.3\text{T}$ and $N_a = 3.16 \times 10^{18}\text{cm}^{-3}$ (\circ) are shown on fig. 1 (also repeated on fig. 2). These can be seen to match remarkably well with the experimental data taken at $N_a = 2.5$ and $7 \times 10^{18}\text{cm}^{-3}$, making it clear that it is important to include the ionised impurity scattering in a model intended to reproduce the experimental value of r_H .

We can conclude that when impurity scattering domi-

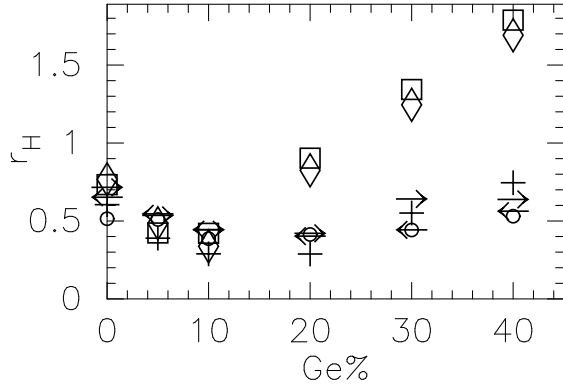


FIG. 3: Hall coefficients for strained $\text{Si}_{1-x}\text{Ge}_x$ alloy, at $B = 1.00\text{T}$, as a function of Ge fraction. **Monte Carlo:** \square = undoped; \diamond = 10^{15}cm^{-3} ; $+$ = 10^{17}cm^{-3} ; \leftarrow = 10^{18}cm^{-3} ; \circ = $3.16 \times 10^{18}\text{cm}^{-3}$; \rightarrow = 10^{19}cm^{-3} . Error bars are not included because the symbols become obscured, but are listed in table II. They are smaller for lower doping concentrations, are typically smaller than ± 0.1 , and are no greater than ± 0.211 .

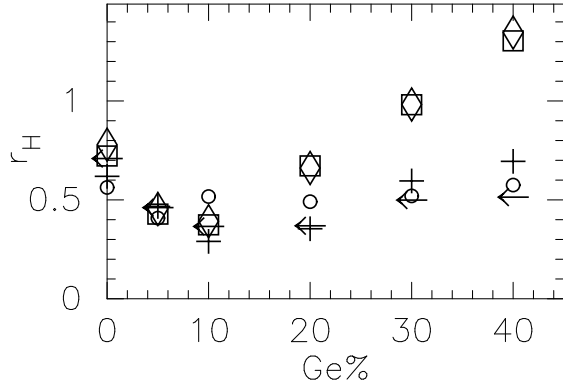


FIG. 4: Hall coefficients for strained $\text{Si}_{1-x}\text{Ge}_x$ alloy, at $B = 2.00\text{T}$, as a function of Ge fraction. **Monte Carlo:** \square = undoped; \diamond = 10^{15}cm^{-3} ; $+$ = 10^{17}cm^{-3} ; \leftarrow = 10^{18}cm^{-3} ; \circ = $3.16 \times 10^{18}\text{cm}^{-3}$; \rightarrow = 10^{19}cm^{-3} . Error bars are not included because the symbols become obscured, but are listed in table II. They are smaller for lower doping concentrations, are typically smaller than ± 0.1 , and are no greater than ± 0.192 .

nates, r_H stays low up to high Ge concentrations, a case which contrasts with that studied by Dykstra, who did not include impurity scattering. Our results thus agree much better with experiment than his – indeed, the importance of impurity scattering was suggested by Dykstra as a reason for the discrepancy he noticed. The full range of r_H values from the Monte Carlo results are shown on figs. 2, 3, 4 for a range of B values. These emphasise the role of impurity scattering – the r_H values in undoped and low doping simulations are significantly higher than those for higher doping.

IV. CONCLUSIONS

Comparison of our Monte Carlo simulation results for doped strained $\text{Si}_{(1-x)}\text{Ge}_x$ with experimental results [1] have clearly shown that ionised impurity scattering has an important role in determining the Hall parameter r_H . This was shown by simulations which without ionised impurity scattering failed to give agreement with experiment, but with it gave good agreement. This was despite using a linearly interpolated set of band parameters, so clearly the interpolation scheme is less important than the impurity scattering mechanism.

Following on from this work, it would be good to reduce the statistical errors in the Hall co-efficients further. This would enable us to make comparisons between different interpolation schemes for the $\text{Si}_{(1-x)}\text{Ge}_x$ parameters. Also, the behaviour of the Hall parameter in relaxed $\text{Si}_{(1-x)}\text{Ge}_x$ would be interesting to consider.

- [*] Electronic mail: Dr.Paul.Kinsler@physics.org
- [1] K.B. Joelsson, Y. Fu, W.X. Ni, G.V. Hansson, J. Appl. Phys. **81**, 1264 (1997).
- [2] Y.C. Chen, S.H. Li, P.K. Bhattacharya, J. Singh, J.M. Hinkley, Appl. Phys. Lett. **64**, 3110 (1994).
- [3] J.E. Dijkstra, *Monte Carlo Simulation of hole transport in Si, Ge, and Si_(1-x)Ge_x*, T.U. Delft (1997).
- [4] J.E. Dijkstra, W.Th. Wenckebach, J. Appl. Phys. **85**, 1587 (1999).
- [5] M.M. Rieger, P. Vogl, Phys. Rev. B. **48**, 14276 (1993).
- [6] M.J. Haye, *A Parallel Car-Parrinello scheme: development and applications*, T.U. Delft (1998).
- [7] F. M. Bufler, P. Graf, B. Meinerzhagen, G. Fischer, H. Kibbel, J. of Vac. Sci. Technol. B **16**, 1667-1669 (1998); ibid. **16**, 2906 (1998).
- [8] M. V. Fischetti, S. E. Laux, J. App. Phys. **80**, 2234-2252 (1996).
- [9] Tsyr-Shyang Liou, Tahui Wang, Chun-Yen Chang, J. App. Phys. **76**, 2234-2252 (1994).
- [10] W.Th. Wenckebach, P. Kinsler, Computer Physics Communications **143**, 136 (2002).
- [11] C. Moglestu, *Monte Carlo simulation of semiconductor devices*, (Chapman & Hall, London, 1993).
- [12] E.O. Kane, in *Semiconductors and Semimetals*, eds. R.K. Willardson and A.C. Beer, (Academic Press, New York, 1966), Vol. **1**, page 75.
- [13] B.K. Ridley *Quantum Processes in Semiconductors*, (Clarendon Press, Oxford, 1988).
- [14] L. Reggiani, in *Hot electron transport in semiconductors*, ed. L. Reggiani, (Springer-Verlag, Berlin, 1985), page 7.
- [15] P. Kinsler, W.Th. Wenckebach, J. App. Phys. **90**, 1692 (2001).
- [16] P. Kinsler, W. Th. Wenckebach, Proc. 25th Internat. Conf. on the Physics of Semiconductors Parts I/II, ICPS-25 Osaka 2000, ed. by N. Miura, T. Ando, Springer Proceedings in Physics. Vol. **87**, pages 711-712 (Springer, Berlin 2001). Also see <http://arXiv.org/abs/cond-mat/0201396>
- [17] J.E. Dijkstra, W.Th. Wenckebach, Appl. Phys. Lett. **70**, 2428 (1997).
- [18] P.J. Briggs, A.B. Walker, D.C. Herbert, Semicond. Sci. Tech. **13**, 680 (1998).
- [19] P.J. Briggs, A.B. Walker, D.C. Herbert, Semicond. Sci. Tech. **13**, 692 (1998).
- [20] J.M. Hinkley, J. Singh, Phys. Rev. B **41**, 2912 (1990).
- [21] P. Kinsler, W.Th. Wenckebach, unpublished.

Parameter	Si	Ge	Units
valence-band structure L	-5.53	-30.53	dimensionless
M	-3.64	-4.64	dimensionless
N	-8.75	-33.64	dimensionless
spin-orbit splitting D_{lo}	0.044	0.300	eV
deformation potential a	2.1	2.0	eV
b	-2.2	-2.1	eV
d	-5.3	-7.0	eV
d_0	29.3	40.0	eV
lattice constant a_0	5.43095	5.6579	Angstrom
elastic stiffness c_{11}	16.56	13.064	10^{11} dyn/cm ²
c_{12}	6.39	4.885	10^{11} dyn/cm ²
c_{44}	7.95	6.857	10^{11} dyn/cm ²
mass density ρ	2.328	5.3243	g/cm ³
optical phonon energy E_{op}	0.063	0.037	eV
dielectric constant ϵ	11.90	15.90	

TABLE I: Material parameters for silicon and germanium, as used in our simulations. They are similar to those used by Hinkley and Singh[20].

Hall co-efficient r_H							
B (T)	Ge%	$\log_{10} N_A \text{ (cm}^{-3}\text{)}$					
		0.0	15.0	17.0	18.0	18.5	19.0
0.30	40	2.417 \pm 0.032	2.056 \pm 0.052	0.725 \pm 0.071	0.464 \pm 0.118	0.687 \pm 0.092	0.761 \pm 0.161
0.30	30	1.820 \pm 0.043	1.496 \pm 0.075	0.493 \pm 0.091	0.358 \pm 0.132	0.471 \pm 0.115	0.717 \pm 0.202
0.30	20	1.157 \pm 0.039	1.017 \pm 0.101	0.297 \pm 0.124	0.466 \pm 0.151	0.440 \pm 0.133	0.494 \pm 0.196
0.30	10	0.456 \pm 0.022	0.475 \pm 0.139	0.244 \pm 0.164	0.240 \pm 0.189	0.513 \pm 0.164	0.637 \pm 0.314
0.30	5	0.408 \pm 0.013	0.253 \pm 0.160	0.402 \pm 0.184	0.373 \pm 0.211	0.557 \pm 0.184	0.715 \pm 0.349
0.30	0	0.737 \pm 0.011	0.726 \pm 0.210	0.601 \pm 0.196	0.597 \pm 0.226	0.642 \pm 0.200	0.493 \pm 0.313
1.00	40	1.788 \pm 0.016	1.691 \pm 0.029	0.745 \pm 0.035	0.563 \pm 0.039	0.531 \pm 0.076	0.638 \pm 0.107
1.00	30	1.343 \pm 0.019	1.245 \pm 0.034	0.551 \pm 0.044	0.443 \pm 0.048	0.442 \pm 0.095	0.641 \pm 0.136
1.00	20	0.903 \pm 0.022	0.825 \pm 0.043	0.288 \pm 0.057	0.403 \pm 0.062	0.413 \pm 0.120	0.421 \pm 0.125
1.00	10	0.421 \pm 0.015	0.337 \pm 0.059	0.289 \pm 0.077	0.444 \pm 0.080	0.387 \pm 0.156	0.444 \pm 0.148
1.00	5	0.423 \pm 0.011	0.485 \pm 0.069	0.390 \pm 0.087	0.545 \pm 0.089	0.509 \pm 0.174	0.536 \pm 0.190
1.00	0	0.733 \pm 0.010	0.767 \pm 0.074	0.605 \pm 0.093	0.652 \pm 0.096	0.514 \pm 0.190	0.716 \pm 0.211
2.00	40	1.304 \pm 0.019	1.346 \pm 0.018	0.695 \pm 0.046	0.514 \pm 0.052	0.575 \pm 0.076	
2.00	30	0.981 \pm 0.021	0.982 \pm 0.025	0.596 \pm 0.064	0.499 \pm 0.078	0.520 \pm 0.095	
2.00	20	0.672 \pm 0.021	0.661 \pm 0.029	0.354 \pm 0.058	0.369 \pm 0.098	0.491 \pm 0.121	
2.00	10	0.374 \pm 0.016	0.392 \pm 0.038	0.290 \pm 0.077	0.366 \pm 0.126	0.517 \pm 0.157	
2.00	5	0.428 \pm 0.013	0.454 \pm 0.044	0.467 \pm 0.110	0.461 \pm 0.141	0.408 \pm 0.174	
2.00	0	0.722 \pm 0.013	0.779 \pm 0.046	0.619 \pm 0.133	0.709 \pm 0.152	0.563 \pm 0.192	

TABLE II: Monte Carlo results for SiGe Hall Co-efficient r_H . A full set of simulation results with data for drift and Hall mobilities, mean energies, time of flight, diffusion, and numbers of blocks required can be found in [21]

Drift Mobility μ_c							
B (T)	Ge%	$\log_{10} N_A \text{ (cm}^{-3}\text{)}$					
		0.0	15.0	17.0	18.0	18.5	19.0
0.30	40	1517.0 \pm 3.18	1457.0 \pm 3.26	931.3 \pm 258.60	478.6 \pm 0.78	391.3 \pm 0.40	388.0 \pm 12.14
0.30	30	1156.0 \pm 3.21	1116.0 \pm 10.23	637.6 \pm 1.08	390.4 \pm 0.57	323.7 \pm 6.41	305.2 \pm 0.52
0.30	20	860.7 \pm 2.26	827.4 \pm 1.94	498.9 \pm 2.60	311.2 \pm 1.52	257.4 \pm 5.49	238.6 \pm 0.30
0.30	10	598.2 \pm 1.31	794.7 \pm 402.90	385.4 \pm 18.17	240.3 \pm 0.35	196.6 \pm 0.18	187.9 \pm 11.53
0.30	5	516.6 \pm 1.08	502.7 \pm 1.06	337.1 \pm 0.61	218.6 \pm 2.44	177.2 \pm 0.16	162.6 \pm 0.25
0.30	0	496.2 \pm 1.20	481.4 \pm 1.28	324.8 \pm 0.61	206.4 \pm 0.28	166.1 \pm 0.16	149.8 \pm 0.19
1.00	40	1309.0 \pm 2.01	1281.0 \pm 3.84	791.8 \pm 2.10	477.4 \pm 0.85	391.3 \pm 1.09	379.0 \pm 1.42
1.00	30	1054.0 \pm 1.91	1032.0 \pm 3.09	633.8 \pm 1.70	403.0 \pm 25.07	318.3 \pm 0.89	304.3 \pm 1.16
1.00	20	816.9 \pm 1.74	795.1 \pm 2.41	495.6 \pm 1.36	309.8 \pm 0.56	286.3 \pm 64.90	238.2 \pm 0.64
1.00	10	587.7 \pm 1.19	575.7 \pm 5.71	376.0 \pm 1.04	241.2 \pm 1.92	196.2 \pm 0.55	182.3 \pm 0.44
1.00	5	510.9 \pm 1.04	507.2 \pm 15.85	337.0 \pm 0.96	217.3 \pm 0.40	177.0 \pm 0.50	162.2 \pm 0.45
1.00	0	492.2 \pm 1.18	478.3 \pm 1.46	324.6 \pm 0.96	205.8 \pm 0.39	165.6 \pm 0.49	149.7 \pm 0.43
2.00	40	1133.0 \pm 3.04	1111.0 \pm 3.31	769.2 \pm 5.06	474.3 \pm 2.23	389.9 \pm 2.18	
2.00	30	946.8 \pm 2.79	929.4 \pm 3.36	622.3 \pm 4.73	388.1 \pm 2.21	317.9 \pm 1.79	
2.00	20	761.3 \pm 2.29	745.5 \pm 2.71	490.7 \pm 2.68	311.8 \pm 6.37	251.5 \pm 1.42	
2.00	10	567.6 \pm 1.70	556.0 \pm 2.01	374.7 \pm 2.08	240.5 \pm 1.37	195.9 \pm 1.11	
2.00	5	499.1 \pm 1.55	488.7 \pm 1.79	333.9 \pm 2.36	216.7 \pm 1.26	178.8 \pm 3.33	
2.00	0	482.8 \pm 1.77	469.0 \pm 1.75	323.6 \pm 2.70	205.5 \pm 1.24	165.3 \pm 0.97	

TABLE III: Monte Carlo results for SiGe drift mobility μ_c .